



## OPEN Research on the extension of respiratory interaction modalities in virtual reality technology and innovative methods for healing anxiety disorders

Shaoting Zeng<sup>1</sup>✉, Liyi Chen<sup>1</sup> & Suihong Lan<sup>2</sup>

The timely alleviation and healing of anxiety is crucial for preventing anxiety disorders. This study explores innovative digital approaches for anxiety relief by integrating virtual reality (VR) and multimodal interaction theories and technologies with psychodrama therapy and breathing therapy from psychology. The research proposes an innovative method of breathing interaction based on olfactory interaction modalities and designs breathing interaction semantics aimed at anxiety healing through three types of breathing therapy. Using the Unreal Engine, VR gamified scenarios and interaction logic for levels were constructed, leading to the development of a multimodal immersive software interaction system and a prototype for VR hardware interaction that extends the breathing interaction modality. The effectiveness of the system for anxiety relief was validated through an EEG experiment involving 38 participants, supported by analysis of Topographic Maps, Band-Power Reports, ERP analysis, and qualitative data from the USE scale. This research confirms that the innovative integration of VR and breathing interaction modalities is effective for anxiety therapy, aiding users in promptly alleviating anxiety and simplifying the psychological healing process.

**Keywords** Anxiety therapy, Virtual reality, Breath interaction, Multimodal interaction, Unreal engine

Anxiety disorder is a mental illness that causes patients to experience pronounced feelings of anxiety and fear<sup>1</sup>. Studies indicate that some patients are more prone to associate ordinary events with negative outcomes<sup>2</sup>. These sensations can lead to physical symptoms, such as tachycardia and trembling. Many scholars believe that the development of anxiety symptoms is closely related to thought and cognitive processes, as well as certain physiological factors. Anxiety among university students is widespread, with the primary causes being interpersonal relationships and concerns about academics and employment. A study utilizing the Self-Rating Anxiety Scale (SAS)<sup>3</sup> surveyed 752 university students regarding their levels of anxiety. The results revealed that 19% of the students exhibited mild anxiety, 3% demonstrated moderate anxiety, and 1% exhibited severe anxiety, totaling 23% of the participants showing signs of anxiety<sup>4</sup>.

As the focus on contemporary mental health continues to heighten, an increasing number of non-pharmacological treatment methods are gaining attention. Research has shown that psychological therapies, such as Cognitive Behavioral Therapy (CBT), are highly effective in treating anxiety disorders. CBT aids patients in identifying and altering negative thought and behavior patterns, alleviating symptoms of anxiety, and enhancing overall mental health<sup>5</sup>. Mindfulness-Based Stress Reduction (MBSR), recognized for its potential to modify cognition and affect emotions, is particularly noteworthy given that anxiety disorders are characterized by emotional and attentional biases as well as distorted negative self-beliefs. Studies have examined changes in the brain associated with MBSR, including behavioral indices of emotional response and the regulation of negative self-beliefs in patients<sup>6</sup>.

Although non-pharmacological interventions have demonstrated significant potential in treating anxiety disorders, further research is required to fully understand their effectiveness and the best methods of implementation. Researchers are exploring novel therapeutic approaches, such as Virtual Reality Exposure Therapy (VRET) and art therapy, as potential treatments for anxiety disorders. VRET allows patients to confront

<sup>1</sup>College of Art and Design, Beijing University of Technology, Beijing 100124, China. <sup>2</sup>Academy of Arts & Design, Tsinghua University, Beijing 100084, China. ✉email: sjmjjst@gmail.com

their fears in a controlled environment<sup>7,8</sup>, while art therapy utilizes creative expression to help patients manage their anxiety symptoms<sup>9,10</sup>.

With the introduction of the metaverse concept and the advancement of related technologies, psychological healing methods incorporating virtual reality have emerged. The metaverse represents a persistent and decentralized online three-dimensional virtual environment, where users can enter a man-made digital world through virtual reality devices<sup>11</sup>. This offers new opportunities and possibilities for personalized and multimodal interaction for psychological healing users<sup>12</sup>. Although the external perception of the metaverse concept and its attributes is still evolving, there is already widespread consensus on the optimistic future prospects of the metaverse. Based on virtual reality and sensor technologies, this study explores innovative methods for anxiety psychological healing through a system of multimodal and immersive interactions.

### Multimodal interaction

Modality is a biological concept introduced by the German physiologist Hermann von Helmholtz, referring to the channels through which organisms receive information via sensory organs and experience<sup>13</sup>. Multimodality refers to the integration of multiple senses. The various senses of the human body provide multiple input and output modes, which together constitute the human sensory system, offering people a rich array of perceptual experiences<sup>14</sup>.

“The eyes, ears, nose, tongue, body, and mind; form, sound, smell, taste, touch, and phenomena” originates from the Heart Sutra, listing all human senses in the language of Chinese traditional culture<sup>15</sup>. “The eyes, ears, nose, tongue, body, and mind” correspond to “vision, hearing, olfaction, taste, tactility, and cognition” respectively. These six sensory organs play a crucial role in human perceptual experiences. Meanwhile, “form, sound, smell, taste, touch, and phenomena” refer to the sensations of “color, sound, odor, flavor, and consciousness” that these six sensory organs can perceive. In virtual reality human-computer interaction, when these modalities are activated simultaneously, users can experience a rich, authentic, and immersive interaction experience<sup>16</sup>.

Multimodal interaction refers to the communication between humans and computers through multiple channels including sound, body language, information carriers (text, images, audio, video), and environment, fully simulating the natural ways of interaction among people<sup>17</sup>. By integrating various sensory input modes through computer technology and using them in combination, a more detailed and enriched experience can be created.

As theoretical and technological advancements mature, research and applications of multimodality in the fields of computer science and artificial intelligence have gradually formed a more mature paradigmatic system<sup>18</sup>. In the development of immersive interaction technologies such as virtual reality (VR) and augmented reality (AR), considering specific needs and user differences, the combination of various sensory input modes can provide a higher quality user experience and a more authentic embodied experience. The research teams at the MIT Media Lab have conducted a series of interdisciplinary studies on psychological healing based on intelligent interaction technologies. The HeartBit project developed a handheld cardiac shape tactile interaction sensor that provides real-time feedback on the user's heart rate to enhance self-awareness and regulate psychological states<sup>19</sup>. The Essence project designed and developed a scent interaction necklace controllable via smartphone, which adjusts the intensity and frequency of essential oil release based on the user's physiological characteristics and sensor data<sup>20,21</sup>. An early research prototype from this project, BioEssence, is a wearable scent display<sup>22</sup>. The authoring team also developed an intelligent interaction product named Lotuscent in the early stages, aimed at helping insomnia sufferers improve their psychological state<sup>23</sup>. The EmBER project is dedicated to developing wearable sensory interaction devices that convey non-verbal signals, thereby enriching remote emotional communication and interaction forms<sup>24</sup>. The AttentivU project combines AR glasses HoloLens 2 with a brain-computer interface system to visualize users' psychological and sustained attention states during immersive interaction experiences<sup>25</sup>. The Baguamarsh project explores integrating personal user data in a virtual reality interaction environment for customized interactions and experiences with environmental data and media information<sup>26</sup>. This study enhances a virtual reality interaction system with a breath interaction modality and integrates it with breathing methods for anxiety therapy, developing an immersive multimodal embodied interaction system based on breath interaction.

### Virtual reality and immersive interaction

Immersive technology refers to a type of technology that enables users to immerse themselves in a virtual environment and interact with it. The development of this technology is driven by the demand for more authentic, in-depth, and personalized user experiences<sup>27</sup>. Immersive technology has a wide range of applications, including entertainment, education, healthcare, design, and more. For example, the game “Half-Life: Alyx” produced by Valve in 2020, utilizes virtual reality technology to present and construct its core gameplay. Players can immerse themselves fully through virtual reality devices, engaging in deep environmental interactions, solving puzzles, exploring the world, and experiencing battles that are almost indistinguishable from reality<sup>28,29</sup>.

#### *Unreal engine*

Unreal Engine, developed by Epic Games, is a game engine that serves as a comprehensive tool for developing interactive systems, suitable for any application employing real-time interaction technologies<sup>30</sup>. This study utilizes Unreal Engine in conjunction with Oculus VR head-mounted hardware devices and Arduino sensors to integrate and construct a multimodal immersive virtual reality interaction system.

Wireless or wired connections through Oculus VR hardware devices enable real-time VR interaction functionalities within Unreal Engine. In terms of facilitating communication between Unreal Engine and

Arduino, the SerialCom4 plugin is used for data transmission. This approach allows for the integration of Arduino breath sensor data into Unreal Engine in this study<sup>31</sup>.

#### *VR headset*

The Meta Quest virtual reality device, developed by Meta's Oculus division, is a VR headset. Quest is an Android-based standalone device capable of running games and software wirelessly. It supports six degrees of freedom in position tracking, primarily using internal sensors and a series of cameras located at the front of the headset. The Oculus Link feature allows Quest devices to connect to an external computer via a data cable, enabling them to run and connect with Unreal Engine systems.

### **Psychodrama therapy**

Psychodrama was introduced by the psychiatrist Jacob L. Moreno in 1921, offering patients a safe environment to explore, release, become aware of, and share their inner selves through experiencing or re-experiencing their thoughts, emotions, and interpersonal relationships within a performance context<sup>32</sup>. During the unfolding of the drama, patients can effectively release emotions through this theatrical form, thereby achieving therapeutic effects. Psychodrama therapy is grounded in behaviorism and humanism<sup>33,34</sup>. Behaviorism posits that human behavior is a response generated by the external environment, meaning behavior is determined by stimuli and responses. Consequently, psychodrama therapy aims to alter patients' behavior and emotions by changing environmental and behavioral stimuli, achieving therapeutic goals. For instance, exposure therapy reduces the intensity of fear by exposing patients to the stimuli that frighten them. Humanism, on the other hand, suggests that humans possess inherent potential for self-actualization and development, and happiness and fulfillment can be obtained through self-realization<sup>35</sup>. Psychodrama therapy facilitates emotional change and healing by helping patients discover and develop their inner potential.

Psychodrama therapy and the concept of the metaverse are interconnected, as both offer a means of simulating scenarios to help users or patients better understand themselves, requiring effective interaction methods and immersion to achieve this goal. Leveraging the high fidelity of virtual reality technology, healthcare professionals can provide patients with a safe, controllable, virtual environment. This aids in allowing patients to experience various situations within a virtual world, thereby alleviating their distress and symptoms<sup>36,37</sup>. Research findings indicate that using virtual reality technology for the psychodrama therapy has shown significantly better outcomes compared to traditional methods, enabling participants to feel a deeper connection with the imagined object.

### **Breath healing methods**

#### *Diaphragmatic breathing technique*

Diaphragmatic breathing is a deep and slow method of respiration that influences the brain and cardiovascular, respiratory, and digestive systems through the regulation of autonomic nervous function. Practitioners should focus on keeping the chest as still as possible during breathing, emphasizing the contraction of the diaphragm. The diaphragm is one of the primary respiratory muscles, and its function is crucial for normal respiration. Research has shown that diaphragmatic breathing can effectively improve the exercise capacity and respiratory function of patients with Chronic Obstructive Pulmonary Disease (COPD)<sup>38,39</sup>. Moreover, this method also aids in stress relief and ameliorates issues such as eating disorders, chronic functional constipation, hypertension, migraines, and anxiety. Additionally, it can enhance the quality of life for cancer and Gastroesophageal Reflux Disease (GERD) patients and promote cardiopulmonary health in individuals with heart failure<sup>40,41</sup>. The diaphragm has multiple physiological functions; notably, the phrenic nerve, which is related to diaphragmatic function, is closely associated with the vagus nerve, impacting the entire body system. The movement of the diaphragm during breathing directly and indirectly affects the sympathetic and parasympathetic nervous systems, as well as motor nerve activity and brain health<sup>42</sup>.

Aerobic exercises such as Tai Chi and yoga utilize diaphragmatic breathing. A study has shown that Tai Chi and yoga can alleviate stress in individuals under high stress or negative emotional states by regulating the balance between the sympathetic and vagus nerves<sup>43</sup>. Diaphragmatic breathing increases post-exercise antioxidant activity and reduces oxidative stress, while also demonstrating positive therapeutic effects on anxiety disorders in assessments. It has the potential to become a non-pharmacological treatment method for patients with anxiety disorders, stress disorders, and chronic respiratory diseases.

#### *Sustained breathing therapy*

Currently, in the medical field, there exist therapies related to sustained exhalation, such as Positive Expiratory Pressure (PEP) therapy, whose primary function is to help expand the airways. Studies have shown that compared to the Active Cycle of Breathing Techniques (ACBT), daily use of a flutter valve PEP therapy for four weeks improves overall health status. It shows certain improvements in alleviating symptoms of breathlessness, coughing, and lung capacity. This healing method is primarily applied in respiratory therapy. Given that symptoms of anxiety disorders often include rapid breathing and difficulty breathing, it is speculated that this healing method, through modification, has the potential to be applied in the treatment of anxiety disorders<sup>44</sup>.

Another method of treatment through sustained exhalation is pursed-lip breathing. This is a rehabilitation training method suitable for patients with Chronic Obstructive Pulmonary Disease (COPD). Additionally, it can also serve as an adjunct measure for patients undergoing exercise rehabilitation or respiratory muscle training. Employing this breathing therapy can facilitate the relaxation of the respiratory muscles, extend the airway opening time, and prolong the exhalation phase<sup>45</sup>.

### Breath-holding therapy

The primary feature of breath-holding therapy is its ability to increase the carbon dioxide content within cells. A deficiency in carbon dioxide can lead to spasms, irritability, dizziness, and nausea, as cells lack carbon dioxide for exchanging the oxygen transported by the blood, in addition to a reduction in the absorption of oxygen into the cells. Holding one's breath allows cells more time to absorb oxygen and produce carbon dioxide. This is why breath-holding sometimes increases the carbon dioxide content in cells and alleviates conditions regulated by hyperventilation, thereby serving to reduce stress and anxiety.

An experimental study on mice has indicated that the increase in the percentage of carbon dioxide in bodily cells, which may occur due to breath-holding, could protect brain cells<sup>46</sup>. Additionally, research on salamanders has shown that an increase in carbon dioxide content accelerates the production of Reactive Oxygen Species (ROS), which are essential for the regeneration of the salamander brain<sup>47</sup>. Therefore, using breath-holding therapy to increase the carbon dioxide content in cells also has the potential to promote the regeneration of new tissue in the brain, thereby protecting brain function<sup>48</sup>.

### Research questions and objectives

In summary, psychodrama therapy is a traditional anxiety treatment method with immersive characteristics, while breath therapy is a modality-based healing approach. The objective of this study is to organically integrate these two traditional therapeutic methods through the combination of VR and sensor technologies, thereby exploring digital innovations for anxiety treatment. The ultimate aim is to develop an accessible and effective immersive multimodal interactive system for anxiety therapy.

## Materials and methods

### Research design

This study opts to integrate the olfactory modality and innovatively proposes the breath interaction modality as the primary mode of human-computer interaction for the system constructed herein, as illustrated in Fig. 1. Firstly, breathing, as a therapeutic method for psychological disorders, has shown significant healing effects on anxiety disorders. There is a substantial body of research indicating the close relationship between breathing activities and emotional experiences<sup>49</sup>. The study suggests a potential mechanism based on physiological changes induced by different emotional states, reflected in changes in cell membrane potential. Negative emotional states such as stress, anxiety, and depression lead to the activation of the sympathetic nervous system, which is due to widespread depolarization throughout the brain and body, while slow, deep breathing and meditation lead to the activation of the parasympathetic nervous system due to widespread inhibition and hyperpolarization. These changes in neuronal cell membrane potential may underlie the neurophysiological mechanisms of emotions, with these membrane potential changes believed to occur throughout the body. Furthermore, breath therapy primarily achieves healing through guiding breathing frequency, offering a natural and direct therapeutic approach with strong feasibility and controllability in terms of technical implementation and cost investment.

Secondly, distinct from traditional olfactory modality scent feedback interactions, breathing can serve as a means for user input to the computer. Utilizing existing breath detection technology allows for the direct and immediate feedback of physiological states through human-computer interaction, thereby addressing the current limitation in virtual reality technology where input is primarily through tactile modality via button touches. The integration of a breath smart hardware module with virtual reality hardware can guide the frequency and method of breathing.

The inherent capabilities of virtual reality devices support the combination of tactile, auditory, and visual modalities, which can serve as the computer's output methods to the user, further enriching the feedback and therapeutic effects of immersive experiences. This method of combining modalities organically integrates therapeutic value, interactivity, and innovation.

### Breath detection technology

In the quest for an accurate and user-friendly method of breath detection to correctly guide breath interaction, this study surveyed existing projects related to breath detection, analyzed their technological applications, and ultimately selected two different detection methods for comparative experimentation. The Masque project utilizes the TSY01 temperature sensor chip for collecting breath data and employs bone conduction headphones to adjust the breathing rhythm through audio playback. The recorded data from this experimental study indicate

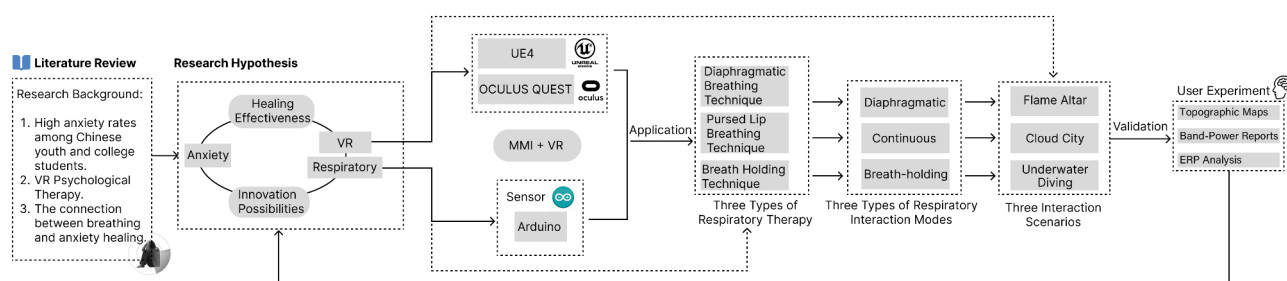


**Fig. 1.** Research workflow and technical approach.

that exhalation is detected when the temperature begins to rise, and inhalation is detected when the temperature starts to drop<sup>50</sup>.

In the Breeze lamp design project, a sound sensor is utilized to detect changes in the loudness of breathing sounds, thereby detecting breaths. Through the variance in sound volume, it exhibits natural methods of lighting and extinguishing, where a gentle blow aids in kindling, and a strong airflow extinguishes the light, linking the intensity of breath with the brightness of the lamp.

This study experimentally compared the effectiveness of temperature (LM75B) and sound (KY-037) sensors for breath detection, finding that changes in detection values could be observed for both sensors during exhalation when monitored through a serial port monitor, while no significant change was observed during inhalation compared to the normal state. However, the temperature detection method exhibited a larger error in the Unreal Engine when storing temperature values as variables for subsequent determination. The sound detection method provided more timely and sensitive feedback in the program. Therefore, based on the experimental results, this study chose the method of using a microphone sensor to detect sounds as the approach for breath detection, see Fig. 2.

The author employed the KY-037 sensor module, which consists of a sensitive electret microphone for detecting sound and an amplification circuit. The module is commonly used to detect sounds exceeding a certain level and is equipped with a potentiometer for setting the noise detection threshold. The analog output voltage varies with the intensity of the sound received by the microphone, allowing this output to be connected to an Arduino analog pin for processing the electrical output<sup>51</sup>.

### Electroencephalogram (EEG) detection technology

#### EEG experimental equipment information

This study utilized the EPOC X device from Emotiv, a 14-channel wireless EEG headset. The device employs saline-based wet sensors, allowing for high-quality EEG data acquisition without the need for adhesive gel. Its lightweight design makes it suitable for integration with VR head-mounted displays in this study. The specific parameters of the device are as follows:

- EEG System: EmotivPRO System.
- Electrode Configuration: The device is equipped with 14 electrodes positioned at AF3, F7, F3, FC5, T7, P7, O1, O2, P8, T8, FC6, F4, F8, and AF4.
- Montage: The electrode placement follows the standard 10–20 system. This study employs a referential montage setup, where signals from each electrode are compared against a common reference electrode, making it suitable for assessing overall emotional states.
- Sampling Rate: The study used a sampling rate of 256 SPS, with an internal sampling rate of 2048 Hz.
- ERP Duration: The ERP analysis focused on EEG activity hundreds of milliseconds before and after an event, with the device supporting an ERP duration of -500 ms to 1000 ms.
- Baseline Correction: Baseline correction is a common preprocessing step in EEG data analysis to eliminate low-frequency drift and noise. In this study, the baseline was set to -500 ms to 0 ms.

#### Topographic maps

Wang et al. found asymmetry in  $\alpha$ -wave power in the prefrontal and parietal regions in individuals with anxiety, with increased activity in the right parietal region being associated with higher levels of anxiety<sup>52</sup>. Stewart's research highlighted that individuals with depression show enhanced left-sided activity in the prefrontal region,

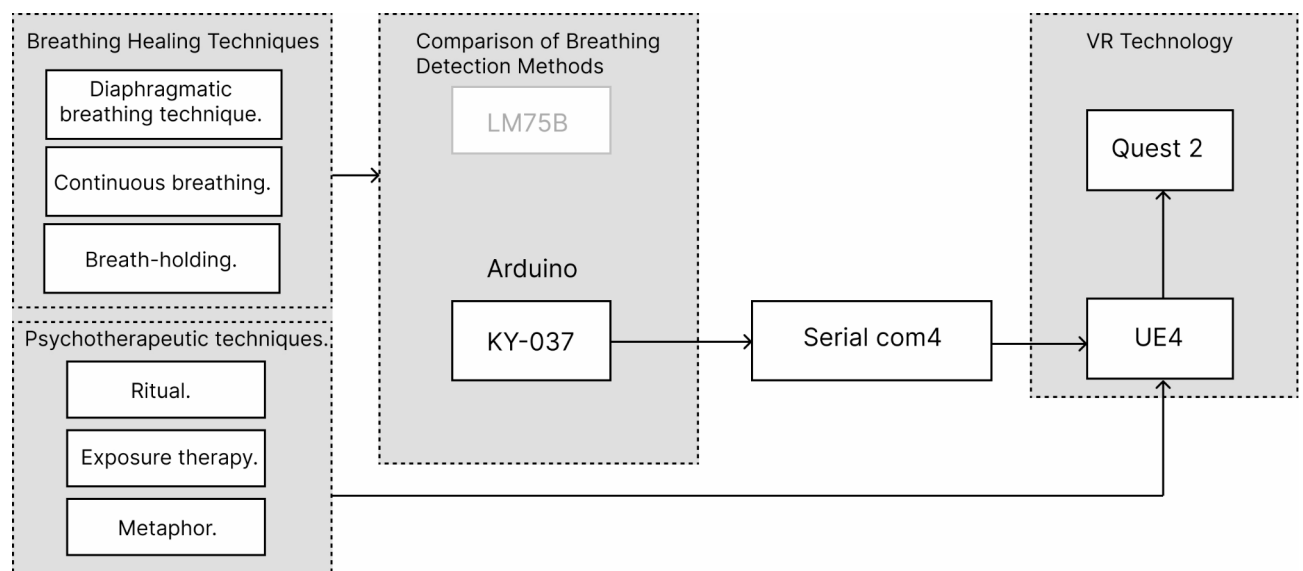


**Fig. 2.** Comparison and selection of breath detection technologies.



particularly during emotional challenge tasks<sup>53</sup>. A review conducted by Palmiero et al. explored prefrontal EEG asymmetry in emotional and mood states, highlighting the differences in prefrontal activity in individuals with anxiety<sup>54</sup>. The research by Metzen et al. assessed the short-term reliability of  $\alpha$ -wave asymmetry in the prefrontal and parietal regions, providing a foundation for understanding the activity differences in these regions in anxious individuals<sup>55</sup>. Monni et al.'s study proposed a prefrontal  $\alpha$ -wave asymmetry factor and examined its correlation with anxiety, depressive symptoms, and personality traits, emphasizing the role of prefrontal activity in emotional regulation<sup>56</sup>.

In summary, through the spatial distribution analysis of EEG, particularly the asymmetry in the prefrontal and parietal regions, the activity differences in these areas in individuals with anxiety were revealed. High-anxiety individuals exhibited increased activity in the right parietal region, while emotional challenge was associated with enhanced activity in the left prefrontal region. These findings confirm the asymmetry of brain activity in anxious states and provide a foundation for the data collection in this study.

**AF3, F3, F4, AF4 (Prefrontal Cortex):** These channels are involved in emotion regulation and control, with noticeable asymmetry in prefrontal activity during anxiety states. AF3 and F3 are typically associated with increased left prefrontal activity, which is linked to anxiety-related worry. In contrast, F4 and AF4 are more closely related to anxiety arousal, reflecting heightened right prefrontal activity. This asymmetry is characterized by enhanced left-sided activity being associated with positive emotions, while increased right-sided activity correlates with anxiety and negative emotions.

**F7, F8 (Temporal Lobes):** In emotion-related EEG studies, F7 (left temporal lobe) and F8 (right temporal lobe) demonstrate differences in emotional processing. The right temporal lobe (F8) shows greater activity in the processing of negative emotions, with individuals experiencing anxiety and stress exhibiting significantly heightened activity in this region.

**P7, P8 (Parietal Lobes):** In anxiety and stress research, the right parietal channel (P8) is more commonly associated with individuals in high-anxiety states. Stress and tension, linked to emotional arousal, trigger a significant increase in right parietal activity.

#### *Band-power reports*

The power spectral density of alpha and beta waves contributes most significantly to anxiety detection, with a particular increase in the beta wave frequency band being highly correlated with anxious states. A reduction in alpha waves and an increase in beta waves are associated with decreased relaxation and heightened tension and anxiety, respectively.

**Alpha Waves (8–12 Hz):** F3, F4: A reduction in alpha wave power in the prefrontal region is associated with anxiety-related worry. P7, P8: A decrease in alpha wave power in the parietal region is linked to anxiety arousal, with this effect being particularly pronounced in the right parietal lobe (P8).

**Beta Waves (13–30 Hz):** F4, P8: An increase in beta wave activity is typically associated with anxiety and stress. Enhanced beta wave activity in the right prefrontal cortex (F4) and right parietal lobe (P8) indicates heightened alertness and elevated levels of anxiety in individuals.

#### *ERP experiment analysis*

ERP experiments are commonly used to capture the instantaneous changes in emotional responses to specific stimuli. Individuals in anxious states typically exhibit stronger ERP responses to negative emotional stimuli, such as threats.

**F3, F4:** In event-related experiments, prefrontal channels (particularly F3 and F4) are used to detect differences in emotional regulation and processing. Anxious individuals show more pronounced ERP responses to negative stimuli in these channels, especially in the P300 and N200 components. Under anxiety conditions, the P300 amplitude in the right prefrontal cortex (F3/F4) is typically reduced, while anxious individuals exhibit a greater N200 amplitude in the F4 channel.

## **Experimental design**

### *Experimental participants*

We used the Zung Self-Rating Anxiety Scale (SAS) to screen participants. The SAS consists of 20 items, including 15 positively scored and 5 negatively scored items, with a four-point rating scale for each<sup>3,57</sup>. Ultimately, 38 participants (19 males and 19 females) with a clear tendency toward anxiety were selected for the experiment. The experimental group included 24 participants (12 males and 12 females), while the control group consisted of 14 participants (7 males and 7 females).

### *Experimental group and control group*

**Experimental Group:** Participants entered the corresponding VR breathing interaction scenarios, during which voice guidance, breathing sound effects, and vibration cues prompted them to engage in breathing exercises. The three scenarios were based on diaphragmatic breathing, extended exhalation, and breath-holding techniques, with environments designed to represent fire, clouds, and the ocean, respectively. Participants received feedback through haptic vibrations on the controllers and visual changes on the screen during the breathing interactions. Each scenario collected data from four breathing cycles per participant, resulting in a total of 12 breathing interaction data points per participant upon completion of the experiment.

**Control Group:** Under the same conditions as the experimental group, participants in the control group were also required to wear all the equipment. However, during the control group experiment, the participants wore the same devices without any VR visual display and did not engage in any interactive operations. They only performed the same breathing cycles as the experimental group. After the same duration as the experimental group, the experiment concluded, and 12 breathing cycle data points were collected from each participant.

*EEG data processing methods*

The EEG data processing involved four steps<sup>58</sup>, labeled A-D, with part of the interface shown on the right side of Fig. 3.

A. Data Preprocessing: The data underwent the following preprocessing steps:

- (1) Re-referencing (corrected using m1/m2).
- (2) Filtering.
- (3) Artifact Correction.

B Topographic Map Generation: To create the topographic maps, we applied spatial interpolation to signals from multiple EEG channels to display the spatial distribution of activity across the scalp. Specifically, we chose the Inverse Distance Weighting (IDW) interpolation method, as it effectively reflects the trend of spatial distribution changes<sup>59</sup>. The workflow involved:

- (1) Data Collection: Electrode potential signals were collected from designated EEG channels (e.g., AF3, F7, F3, etc.).
- (2) Average Potential Calculation: The average potential for each channel was calculated within a defined time window (Eq. 1), where  $V_i(t)$  represents the EEG potential at time  $t$ , and  $N$  is the number of sampling points.

$$V_{avg}(t) = \frac{1}{N} \sum_{i=1}^N V_i(t) \quad (1)$$

3. Interpolation Calculation: Using the Inverse Distance Weighting (IDW) method, the potential value of each electrode was extended to the entire scalp area (Eq. 2), where  $V(x, y)$  represents the potential value at scalp location  $(x, y)$ ,  $V_i$  is the potential value of the  $i$ -th electrode, and  $d_i$  is the distance from location  $(x, y)$  to the  $i$ -th electrode.

$$V(x, y) = \frac{\sum_{i=1}^N \frac{V_i}{d_i^2}}{\sum_{i=1}^N \frac{1}{d_i^2}} \quad (2)$$

- (4) Topographic Map Generation: These interpolated potentials were used to create a scalp potential distribution map, illustrating the activity levels across different regions.

C. To calculate the power of different frequency bands (such as alpha and beta waves), we used the Fast Fourier Transform (FFT) to convert the time-domain signals into frequency-domain signals. The power of specific frequency bands was quantified through Power Spectral Density (PSD)<sup>60</sup>. The workflow included the following steps:

1. Data collection: Raw EEG time-domain signals were collected from the EEG channels
2. Fourier Transform: FFT was applied to the signals, converting the time-domain signals into frequency-domain signals (Eq. 3), where  $X(f)$  is the frequency-domain signal,  $x(n)$  is the time-domain EEG signal,  $N$  is the number of sampling points, and  $f$  represents the frequency.

$$X(f) = \sum_{n=0}^{N-1} x(n) e^{-i2\pi f n/N} \quad (3)$$

3. Power Spectral Density Calculation: Based on the FFT results, the power at frequency  $f$  was calculated (Eq. 4), where  $P(f)$  represents the power at frequency  $f$ , and  $X(f)$  is the FFT result corresponding to that frequency.



**Fig. 3.** Experimental space.

$$P(f) = \frac{|X(f)|^2}{N} \quad (4)$$

4. Bandwidth Power Calculation: The total power within the frequency range of interest (e.g., alpha waves 8–12 Hz) was calculated by integrating the power over this range (Eq. 5), where  $f_1$  and  $f_2$  represent the lower and upper limits of the frequency band.

$$P_{band} = \int_{f_1}^{f_2} P(f) df \quad (5)$$

5. Frequency Band Analysis Report: The power values for each channel across different frequency bands were generated, producing the power spectral report.

D. For ERP analysis, we used the time-locked averaging method, which averages the event-related EEG signals across multiple trials to eliminate background noise and highlight changes in event-related potentials (such as P300). We also calculated the peak amplitude and latency of the event response<sup>61</sup>. The workflow was as follows:

(1) Data Collection: EEG signals before and after the event were collected from multiple channels, locking onto the moment of the event occurrence.

(2) Time-Locked Averaging: The event-synchronized EEG signals from all trials were averaged to extract the event-related potential (ERP) (Eq. 6), where  $V_i(t)$  is the EEG potential from the  $i$ -th trial,  $N$  is the number of trials, and  $ERP(t)$  is the average ERP signal at time  $t$ .

$$ERP(t) = \frac{1}{N} \sum_{i=1}^N V_i(t) \quad (6)$$

3. Peak Calculation: The peak of the ERP waveform was identified within a predefined time window (e.g., 200–400 ms) (Eq. 7), where  $t_1$  and  $t_2$  define the time window after the event, and  $V_{peak}$  represents the maximum potential value.

$$V_{peak} = \max_{t_1 \leq t \leq t_2} |ERP(t)| \quad (7)$$

4. Latency Calculation: The time point at which the peak occurs is identified to calculate the latency (Eq. 8). Latency refers to the time at which the ERP peak appears and is commonly used to assess the brain's response speed.

$$Latency = \arg \max_{t_1 \leq t \leq t_2} |ERP(t)| \quad (8)$$

5. ERP Analysis Results Output: An experimental analysis report is generated, containing key metrics such as ERP amplitude and latency. This report is typically used to analyze the brain's responses to different emotional stimuli.

### Analysis of variance

Analysis of Variance (ANOVA) is a statistical method used to determine whether the differences in means among multiple groups are statistically significant. In this study, ANOVA was employed to statistically analyze the experimental data obtained from Band-Power Reports and ERP. ANOVA decomposes the total variance of the data into two components:

10. (1) Between-Group Variance: This reflects the differences between the means of different groups and represents the variation caused by experimental treatments or group effects.
11. (2) Within-Group Variance: This reflects the random fluctuations within a single group, representing variation caused by individual differences or random error.

By comparing the ratio of these two types of variance (between-group variance and within-group variance), the F-test determines whether the differences in group means are statistically significant.

The calculation steps and formulas for Analysis of Variance (ANOVA) are as follows:

1. Total Variance (SST - Sum of Squares Total)

$$SST = \sum_{i=1}^k \sum_{j=1}^{n_i} (X_{ij} - \bar{X})^2 \quad (9)$$

Where  $X_{ij}$  represents the  $j$ -th sample value in the  $i$ -th group,  $\bar{X}$  denotes the overall mean,  $k$  is the number of groups, and  $n_i$  is the sample size of the  $i$ -th group.

2. Between-Group Variance (SSB - Sum of Squares Between): Represents the variance caused by the deviation of group means from the overall mean.

$$SSB = \sum_{i=1}^k n_i (\bar{X}_i - \bar{X})^2 \quad (10)$$



Where  $\bar{X}_i$  represents the mean of the  $i$ -th group, and  $n_i$  denotes the sample size of the  $i$ -th group.

3. Within-Group Variance (SSW - Sum of Squares Within): Represents the variation among individuals within each group.

$$SSW = \sum_{i=1}^k \sum_{j=1}^{n_i} (X_{ij} - \bar{X})^2 \quad (11)$$

4. Degrees of Freedom (df).

Between-Group Degrees of Freedom:

$$df_{between} = k - 1 \quad (12)$$

Within-Group Degrees of Freedom:

$$df_{within} = N - k \quad (13)$$

Where  $N$  represents the total sample size.

5. Mean Square (MS).

Between-Group Mean Square (MSB):

$$MSB = \frac{SSB}{df_{between}} \quad (14)$$

Within-Group Mean Square (MSW):

$$MSW = \frac{SSW}{df_{within}} \quad (15)$$

6. F-Value calculation

$$F = \frac{MSB}{MSW} \quad (16)$$

Where a larger  $F$ -value indicates more significant differences between groups.

Finally, statistical significance is determined by evaluating whether the differences are significant based on the  $F$ -value and  $p$ -value. The  $F$ -value corresponds to a specific  $F$ -distribution, and the significance level ( $p$ -value) is obtained by comparing the calculated  $F$ -value with the critical value of the  $F$ -distribution. If  $p < \alpha$  (commonly  $\alpha = 0.05$ ), the differences between groups are considered statistically significant.

### Experimental space design

As shown on the left side of Fig. 3, the experimental space design for this study involved participants wearing a VR headset and a 16-channel EEG monitoring device while seated in the central area of the experimental space. The research staff were seated nearby in a designated work area, where they operated computers for data collection and provided real-time assistance to participants throughout the experiment to ensure smooth progress. Additionally, a projector was set up in the experimental space to project the participants' VR headset displays in real-time, allowing the staff to observe the interaction process.

### Results

The therapeutic process designed in this study is divided into three stages, as shown in Fig. 4. In the first stage, users wear VR headset and breath sensor hardware, and run the program. In the second stage, on the selection menu page, users autonomously choose among three different therapeutic methods based on prompts and introductions, according to their needs. In the third stage, after entering the corresponding therapeutic space based on the user's choice from the previous stage, the process and rules are introduced. Once confirmed, the session begins. Users need to adjust their breathing rate and method according to the process rules, and interact with objects in the scene with the aid of vibrations and sounds to complete tasks. Different feedback results are presented upon success or failure, and users can choose to continue or end the therapy.

### Breath interaction modality

To clarify the visual representation of the therapeutic process in virtual reality, this study summarizes and explores natural interaction patterns observed in everyday life, such as blowing out flames, diving, and dispersing smoke. The aim is to discover the optimal way to apply breath healing methods in virtual reality scenarios for interactive therapy, extracting the most familiar and direct subjective sensations from natural interactions and further exploring their relationship with the interactive process. Ultimately, blowing out flames, dispersing clouds, and diving were selected as the final three interactive scenarios, integrating related elements into the design to create intuitive visual feedback.

Integrating virtual reality and Arduino smart sensor technology, this study designs an immersive guidance method for breath interaction. Users are guided in breath interaction through the visual interface of the scene, as well as auditory and tactile modalities. The sensor detects the user's breathing activity, inputting data into the Unreal Engine to facilitate interaction within the virtual scene. Feedback is provided to the user in the VR

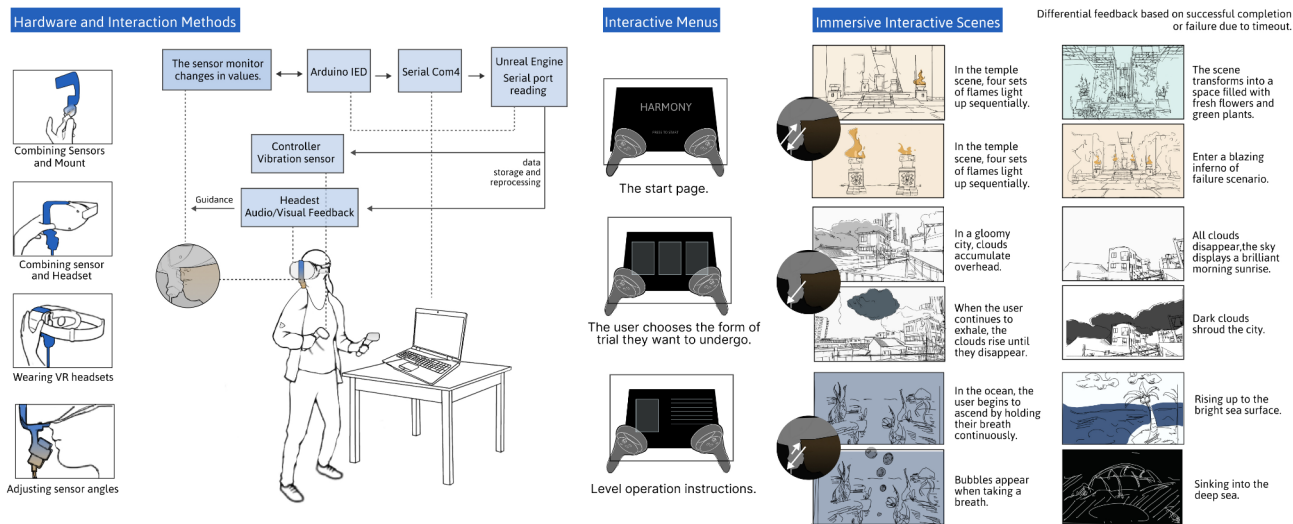


Fig. 4. Interactive system overall architecture and user workflow.

Virtual scene design						
Scene name	Breath interaction	Healing effect	Interactive semantics	Challenge failed	Initial state	Challenge successful
Flame Altar	↑↑↑ ↓↓↓	 Stimulate the parasympathetic nervous system to alleviate neural activity triggered by negative emotions.	 Calm and composed			
Cloud City	↑ ↓ ...	 Enhance lung function and respiratory muscle capacity.	 Continuously output to counter negative emotions.			
Underwater Diving	↑ X ↑	 Regulate excessive ventilation, increase cellular carbon dioxide content, and protect brain cells.	 Maintain a secure state, sustainable sense of security.			
Interactive hardware design						
Arduino Development Board	KY-037 Sensor	Sensor and VR Glasses Connection Structure		Sensors and VR Glasses Wearing Method		

Fig. 5. Interactive system overall architecture and user workflow.

headset through visual modalities. Through gamified level transitions and reward measures, users are guided to complete the entire breath healing process.

As illustrated in Fig. 5, this study proposes a set of breath modality interaction semantics for three breath healing methods, applied within the system. The cycle breathing method based on diaphragmatic breathing stimulates the nervous system and alleviates negative emotions, with its interaction semantics summarized as peace and calmness, and the interaction method being slow inhalation and exhalation. The sustained exhalation method enhances lung function and the level of respiratory muscles, with interaction semantics of continuous output and combating negative emotions, and the interaction method being short inhalation and slow exhalation. Breath-holding adjusts for hyperventilation, increases the carbon dioxide content in cells, and protects brain cells, with semantics of maintaining a safe state and a sustainable sense of security, and the interaction method being continuous exhalation without inhalation.

Virtual reality immersive interaction scenarios

During the process of scenario design, the concepts of flames, oceans, and clouds were used as keywords for extended design. These concepts correspond to the three types of breath healing methods, allowing users

to choose based on their own needs. Each level is designed with a main scene as well as success and failure transition scenes, as illustrated in Fig. 5.

#### *“Flame altar” diaphragmatic breathing interaction scene*

The first level is themed “Flame Altar” corresponding to the diaphragmatic breathing method in breath therapy. The scene is set at an ancient altar surrounded by flames, with intense sunlight streaming from above, creating a hot and scorching atmosphere. Users interact with the flames in the scene through exhalation, following guided steps to progressively extinguish the flames via cyclic breathing. Upon successful completion of this level, the scene transitions to a success scenario. In the design of the success scene, the original flames are replaced with flowers, green plants, and waterfalls, correlating with the comfort felt after successful healing. Conversely, the failure scene incorporates more flames as a gamified penalty for not extinguishing the flames in time.

The specific interaction process is as follows: At the start of the level, the first flame lights up. The user then uses the controller pointer to click on the corresponding torch, which triggers the playback of a breathing guidance audio and controller vibration. Next, the user follows the guide to perform cyclic breathing. Through the sensor, volume data is transmitted to Unreal Engine. In Unreal Engine’s level program, communication ports and baud rates are set using blueprint nodes provided by the SerialCom plugin, and new variables are created to store the data. This data is compared to a fixed value to determine whether breathing activity is currently occurring. When the determination is true, a timer is set using a delay function, and variables are used for timing. Conditions are continuously accumulated until a preset value is reached, extinguishing the flame and completing a cycle of breathing for the user. If not successful, the user can repeatedly click the torch for hints and try again. When the first flame is detected to be extinguished, the second flame lights up, and the process is repeated. After each flame is extinguished, a variable is incremented until all flames are extinguished, leading to a success screen. A timer starts with each lighting of a flame; if the flame is not extinguished within 30 s, it is considered a failure, leading to a failure screen.

#### *“Cloud City” continuous breathing interaction scene*

The second level is themed “Cloud City” corresponding to the sustained exhalation method in breath therapy. The scene depicts a cityscape filled with skyscrapers, with a generally grey tone, and the abundance of tangled cables and distant stations illustrates the anxiety brought about by urban life. The clouds in the scene, as interactive objects, resonate with the semantics of “continuous output, combating negative emotions.” When users follow the guidance to perform sustained exhalation in the level, they disperse the dark clouds hanging over the city. Only continuous exhalation can provide enough power to scatter the clouds. The feedback scene for successful completion of the level is designed as a city under a clear blue sky with clouds, with the messy wires removed, offering users a sense of clarity and emotional relief after healing, resonating with the feedback of the scene. Conversely, if users fail the level, the entire city falls into a dark atmosphere shrouded in dense clouds.

The specific interaction process is as follows: At the start of the level, sound effects and vibration cues automatically play, prompting the user to perform a sustained exhalation after inhaling. The sensor detects this and transmits volume data to Unreal Engine, where new variables are created to store this data. The cloud components are set to be movable and are given simulated physical properties. Multiplying the volume values by a fixed value, a force is applied to the cloud components on the z-axis, having previously set the cloud components to be movable and to simulate physical properties, allowing the clouds to move on the z-axis, creating the effect of being blown away. When exhalation stops and the value decreases, the relative force lessens, causing the clouds to fall. Once the clouds reach a certain height and begin to collide with collision boxes placed in the virtual scene, the clouds disappear. When the current cloud state is determined to be invisible, force begins to be applied to the next cloud. After all eight clouds disappear in sequence, the level is successfully completed, leading to the success screen. A timer starts at the beginning of the level; if the success conditions are not met within one hundred seconds from the start, the level transitions to the failure screen.

#### *“Underwater diving” breath-holding interaction scene*

The third level, themed “Underwater Diving” corresponds to the sustained breath-holding method in breath therapy. The scene is set under the sea, where bubbles are produced in the scene when users exhale, simulating the breath-holding experience while diving and maintaining a safe state underwater by holding one’s breath. In this level, when users maintain a breath-holding state, they can float towards the surface, with the breath-holding state resonating with the semantics of “a sustainable sense of safety.” Upon successful completion of the level, the scene transitions to a calm sea surface after surfacing, representing the relief of being rescued and surfacing successfully. However, failure to complete the level transitions to a failure scene, sinking into the dark abyss of the ocean floor.

The specific interaction process is as follows: At the start of the level, sound effects and vibration cues automatically play. Users inhale and then continue to hold their breath for the duration of the level, which lasts fifty seconds. In this level, users have two opportunities to breathe again. When users exhale and the volume value exceeds a preset threshold, bubble particles appear, creating an exhaling bubble effect on the screen. If the number of breaths exceeds two, the attempt is considered a failure, leading to the failure screen. If it does not exceed two, the environmental brightness is gradually increased through a delay setting while continuously holding breath, brightening the level environment until successfully completed, at which point the success screen is displayed.

### **Hardware and sensors**

As shown in Fig. 6, the breath sensor casing is divided into two parts: left and right. The left part has a protruding insert board that, through the elasticity of the material, achieves an interference fit, connecting with the right

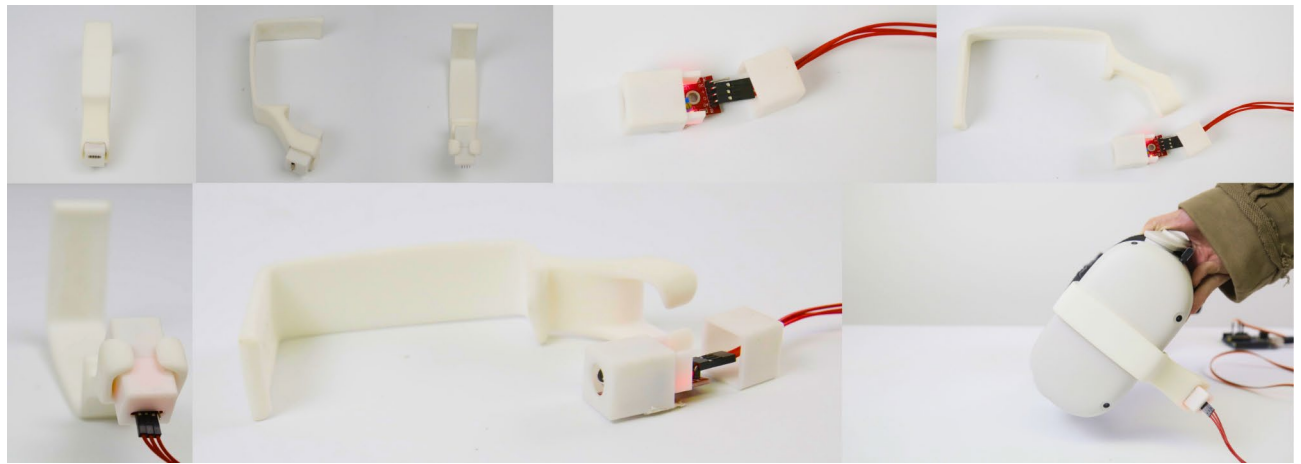


**Fig. 6.** Sensors and related hardware accessories.

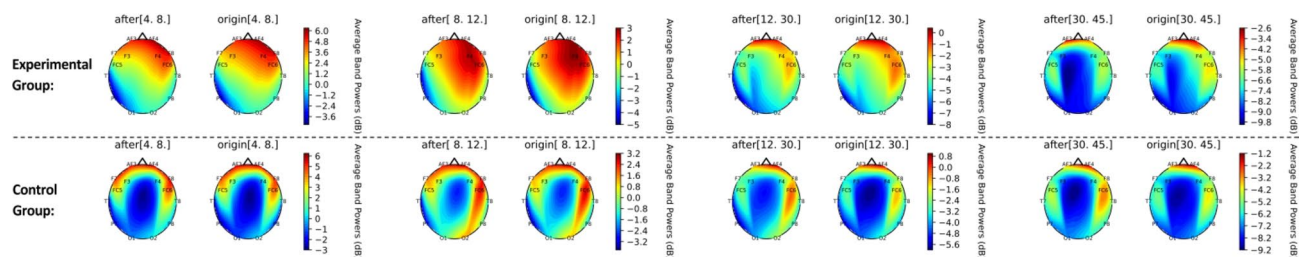


**Fig. 7.** Topographic map analysis results.

side. The plug-in assembly scheme offers rapid and convenient assembly, with a simple structure to facilitate the disassembly and maintenance of the sensor. The use of a mortise and tenon assembly structure without screws also ensures a smooth and regular outer surface, which is beneficial for integration with the connecting bracket structure.

The design of the connecting bracket adopts a structure that can be fixed to the VR glasses and freely detached at any time, used to secure the breath sensor casing. Through a stable structure, the accuracy of the position is ensured, preventing discomfort caused by direct contact of the sensor with the user's face and minimizing the impact on breathing comfort. At the same time, the connection with the VR glasses and the sensor is based on the material's own elasticity, achieved through slot and snap structures, maximizing the simplicity and ease of use of the structure.

When using this product, first push the sensor upwards into the slot; after the sensor is securely fixed, attach the bracket to the VR glasses device; once fixed, the VR glasses device can be worn normally. To enhance measurement accuracy and wearing comfort, the position and angle can be adjusted up and down according to individual needs.

## EEG results from user experiment

### Topographic map analysis results

In the comparison of Topographic Maps (see Fig. 7), a clear elevation in the potential values of the right prefrontal and parietal regions, particularly in the F4 and P8 channels, was observed in the control group. This indicates heightened neural activity in these areas, closely associated with increased anxiety. These findings align with the theory of increased right-sided brain activity during anxiety states, suggesting that the control group did not effectively alleviate anxiety.

In contrast, the experimental group exhibited a significant reduction in potential values in the right prefrontal and parietal regions, particularly in the F4 and P8 channels, with a marked decrease in Topographic Map values. This indicates that, following the intervention, anxiety-related activity in the right prefrontal and parietal regions was significantly alleviated, leading to a reduction in anxiety levels. The decrease in prefrontal asymmetry further supports the improvement in anxiety states.

### Band-power reports analysis results

In the band-power report (see Fig. 8), the power spectral density of alpha waves (8–12 Hz) and beta waves (12–25 Hz) was analyzed in detail. Both control and experimental group showed an increasing trend in alpha



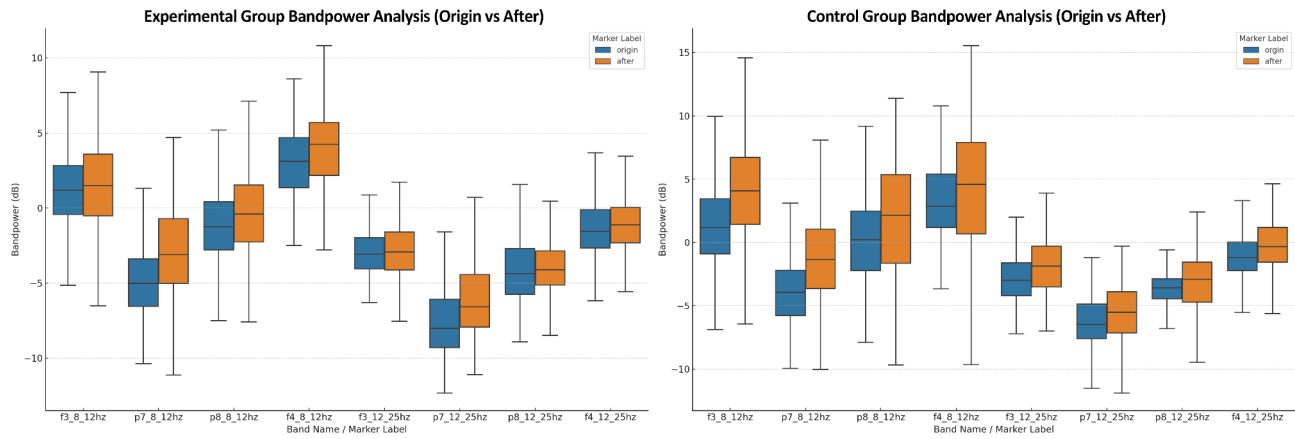


Fig. 8. Band-power reports analysis results.

Electrode position	Frequency band	Time point comparison	F value	Degrees of freedom (df)	p Value	Significance
F3	Alpha (α)	Origin vs. After	5.24	(1, 36)	0.028	Significant
F3	Beta (β)	Origin vs. After	2.45	(1, 36)	0.120	Not Significant
F4	Alpha (α)	Origin vs. After	6.38	(1, 36)	0.017	Significant
F4	Beta (β)	Origin vs. After	4.85	(1, 36)	0.032	Significant
P7	Alpha (α)	Origin vs. After	4.36	(1, 36)	0.023	Significant
P7	Beta (β)	Origin vs. After	1.82	(1, 36)	0.138	Not Significant
P8	Alpha (α)	Origin vs. After	6.72	(1, 36)	0.013	Significant
P8	Beta (β)	Origin vs. After	3.41	(1, 36)	0.029	Significant

Table 1. Analysis of variance on band-power reports experimental data.

wave power spectral density. This aligns with the theory that individuals with anxiety experience an increase in alpha waves as they attempt to regulate emotions and restore a relaxed state.

However, the increase in alpha wave power spectral density in the experimental group was significantly greater than that of the control group, especially in the F3 and F4 channels. This indicates a stronger relaxation response and greater anxiety relief in the experimental group. In contrast, although both groups exhibited a slight increase in beta wave power spectral density, the experimental group's increase was lower than that of the control group, particularly in the right prefrontal and parietal regions. The reduction in beta waves suggests that the experimental group experienced more effective relief from alertness and tension, further demonstrating the experimental group's advantage in anxiety regulation.

The power of different frequency bands (α waves and β waves) at distinct time points (“Origin” and “After”) was compared using boxplots, with power values expressed in decibels (dB). Statistical analyses were conducted to verify the differences in the distribution of band power across channels between the two time points.

This study conducted an analysis of variance (ANOVA) on the changes in α-wave and β-wave power at the F3, F4, P7, and P8 electrode sites between the “Origin” and “After” time points. All analyses were performed using SPSS, with Bonferroni correction applied for p-value adjustments. Table 1 presents the ANOVA results for the Band-Power Reports experimental data, with key statistical findings summarized as follows:

1. F3 Electrode.  
α-wave: The experimental group exhibited a significant increase in α-wave power at the “After” time point ( $F(1, 36) = 5.24, p = 0.028$ ), indicating an enhanced relaxation response following anxiety regulation.  
β-wave: No significant difference in β-wave power was observed between the experimental and control groups ( $F(1, 36) = 2.45, p = 0.120$ ).
2. F4 Electrode.  
α-wave: The experimental group showed a significant increase in α-wave power at the “After” time point ( $F(1, 36) = 6.38, p = 0.017$ ), further supporting the role of anxiety regulation in enhancing relaxation.  
β-wave: A significant decrease in β-wave power was observed in the experimental group ( $F(1, 36) = 4.85, p = 0.032$ ), suggesting a reduction in anxiety-related vigilance.
3. P7 Electrode.  
α-wave: The experimental group exhibited a significant increase in α-wave power at the “After” time point ( $F(1, 36) = 4.36, p = 0.023$ ), further indicating the effectiveness of anxiety alleviation.  
β-wave: Although β-wave power showed a slight increase, the change did not reach statistical significance ( $F(1, 36) = 1.82, p = 0.138$ ).
4. P8 Electrode.



$\alpha$ -wave: The experimental group demonstrated a significant increase in  $\alpha$ -wave power at the “After” time point ( $F(1, 36) = 6.72, p = 0.013$ ).

$\beta$ -wave: The  $\beta$ -wave power in the experimental group decreased compared to the control group, though the significance level was relatively low ( $F(1, 36) = 3.41, p = 0.029$ ).

### 5. Summary.

The significant increase in  $\alpha$ -wave power suggests that the anxiety regulation intervention effectively enhanced relaxation responses. Meanwhile, the decrease in  $\beta$ -wave power, particularly at the F4 electrode site, indicates reduced vigilance. These findings support the critical role of the prefrontal and parietal regions in anxiety regulation.

## ERP analysis results

Through ERP data analysis (see Fig. 9), differences in the N200 and P300 components between the two groups can be observed. The N200 component is primarily associated with cognitive conflict and emotional response. The results indicate that the experimental group exhibited a significant reduction in N200 amplitude, with a decrease notably greater than that of the control group, particularly in the F4 channel. This suggests that the experimental group experienced reduced sensitivity to negative emotions, decreased cognitive conflict, and a greater degree of anxiety relief.

In contrast, the P300 amplitude did not show significant differences between the experimental and control groups, and no clear pattern of change was found. This suggests that during anxiety regulation, the P300 component may not serve as a primary indicator, whereas the N200 component more effectively reflects changes in anxiety.

This study also conducted an ANOVA on the ERP experimental data, with the results presented in Table 2. The key statistical findings are summarized as follows:

### 1. F4 Channel.

**N200 Amplitude:** The experimental group exhibited a significant reduction in N200 amplitude at the “After” time point ( $F(1, 36) = 5.24, p = 0.028$ ), indicating a weakened anxiety response and reduced sensitivity to cognitive conflict and negative emotions following anxiety regulation. In contrast, the control group showed no significant change in N200 amplitude.

**P300 Amplitude:** No significant difference in P300 amplitude was observed between the experimental and control groups at the F4 channel ( $F(1, 36) = 1.87, p = 0.134$ ), suggesting that anxiety alleviation was primarily

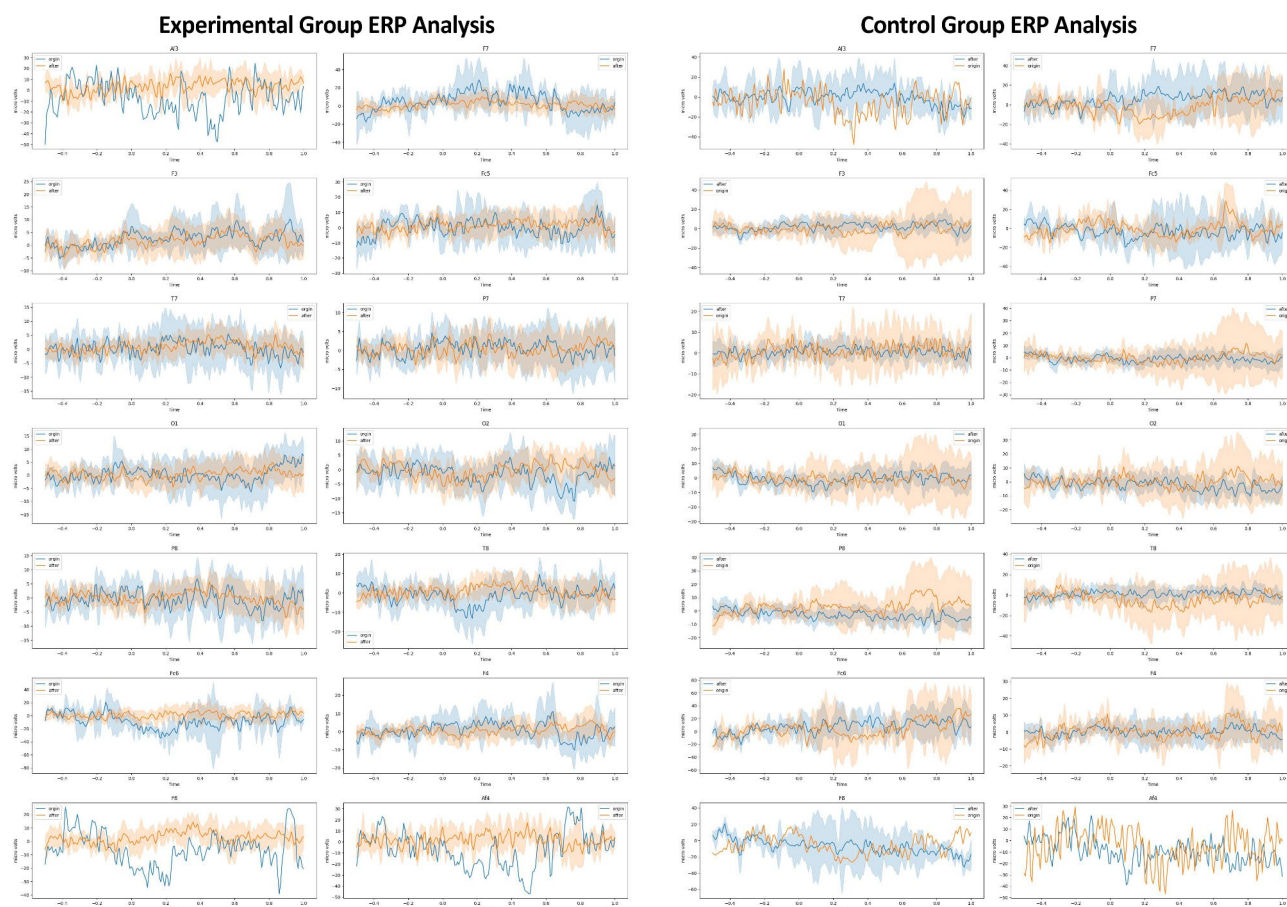


**Fig. 9.** ERP analysis results.

Electrode position	Wave type	Time point comparison	F value	Degrees of freedom (df)	p value	Significance
F4	N200	Origin vs. After	5.24	(1, 36)	0.028	Significant
F4	P300	Origin vs. After	1.87	(1, 36)	0.134	Not Significant
Other Channels	N200	Origin vs. After	< 3.0	(1, 36)	> 0.05	Not Significant
Other Channels	P300	Origin vs. After	< 3.0	(1, 36)	> 0.05	Not Significant

**Table 2.** Analysis of variance on ERP experimental data.

reflected in changes in the N200 component, while P300 amplitude may not be a primary indicator of anxiety regulation.

2. Other Channels.

At other electrode sites, N200 amplitude changes in both the experimental and control groups did not reach statistical significance ( $p > 0.05$ ).

P300 amplitude showed no significant changes across all channels ( $p > 0.05$ ), further indicating that N200 amplitude is a more sensitive marker of anxiety regulation, whereas P300 amplitude may be less reflective of anxiety-related state changes.

3. Summary.

The critical role of N200 amplitude in anxiety regulation was further confirmed, while P300 amplitude did not exhibit significant changes. These findings suggest that anxiety regulation may primarily affect cognitive conflict processing (N200) rather than the later-stage allocation of cognitive resources (P300).

**Experiment summary**

Through the analysis of Topographic Maps, Band-Power Reports, and ERP data, the experimental group demonstrated significant anxiety-relieving effects across all indicators. Specifically, the experimental group exhibited a marked reduction in activity in the right prefrontal and parietal regions, indicating effective suppression of anxiety-related neural activity. In the power spectral report, the experimental group showed a larger increase in alpha wave power, reflecting a stronger relaxation response, while the smaller increase in beta waves pointed to lower levels of alertness and tension. In terms of ERP components, the experimental group's N200 amplitude was significantly reduced, indicating a weakened response to negative emotional stimuli and improved emotional regulation capacity.

These results not only demonstrate that the experimental group outperformed the control group in anxiety relief but also further confirm the neurophysiological observability of emotion regulation and anxiety management. Through the comprehensive analysis of various EEG indicators, we gained a deeper understanding of the activity patterns in different brain regions during anxiety states, as well as the mechanisms of frequency band power and event-related potential changes during emotional regulation. This finding provides neurobiological evidence for future anxiety treatment interventions, suggesting that neuroregulation techniques can more precisely monitor and modulate anxiety states.

On a broader application level, this study not only offers new insights into the neural mechanisms of anxiety but also provides objective and quantifiable biomarkers for anxiety management interventions. This implies that future anxiety treatments can be optimized based on real-time EEG feedback, further enhancing the effectiveness of personalized treatment plans. The potential applications of this approach are wide-ranging, with significant implications for mental health management, clinical interventions, and brain-computer interface technologies.

Thus, this experiment not only confirmed the critical role of EEG data in emotion regulation but also offered new insights into the interdisciplinary integration of neuroscience and psychology. Future research can further explore how precise neuroregulation techniques can more effectively intervene in and manage anxiety, advancing the precision and personalization of anxiety treatment.

**Qualitative report on user experience**

As a supplement to the above EEG experiment data analysis, a user experience survey was conducted with 24 participants from the experimental group out of the total 38 participants to gather additional qualitative feedback on the healing experience. The participants were invited to complete the USE Questionnaire (Usefulness, Satisfaction, and Ease of Use), as shown in Table 3. The USE questionnaire is divided into four dimensions: Effectiveness, Usability, Learnability, and Satisfaction, comprising 30 questions. Each question is rated on a 7-point scale ranging from “strongly disagree” to “strongly agree.” The feedback data from the questionnaire was used for a qualitative assessment of the user experience of the psychological healing interaction system.

The rightmost column of Table 3 presents the average scores of user feedback collected via the USE questionnaire. Qualitative evaluations allow for a rapid understanding of the strengths and weaknesses of the healing experience. For example, the items “I am satisfied with it” and “It is good” achieved average scores exceeding 6, indicating a high level of user satisfaction with the healing system. However, the items “I can use it without a manual” and “I feel that I need to own it” received relatively lower average scores. This suggests that improvements in usability will be necessary during the subsequent product development phase, providing critical insights for the future commercialization and user experience optimization of this research.

**Virtual reality interaction modalities for anxiety psychological healing**

This study leverages virtual reality (VR) technology to design and develop an interactive system aimed at anxiety psychological healing, incorporating breathing therapy to extend the system's breathing interaction modality

Survey questions	Questionnaire score options	Average score results
Effectiveness	Disagree 1 2 3 4 5 6 7 Agree	
It makes my work more effective.		5.88
It makes my work more beneficial.		5.50
It is useful.		5.96
It gives me more control to manage activities in life.		5.41
It enables me to complete tasks more easily.		5.54
When used, it saves me time.		5.50
It meets my needs.		5.54
It can perform all the things I expect it to do.		5.54
Usability	Disagree 1 2 3 4 5 6 7 Agree	
It is easy to use.		6.00
It operates simply.		5.92
It is user-friendly.		5.96
It accomplishes tasks with as few steps as possible.		5.79
It is flexible.		5.54
Using it is effortless.		5.67
I can use it without a manual.		5.38
I didn't find any inconsistencies while using it.		5.46
Both occasional and regular users will like it.		5.58
When errors occur, I can recover quickly and easily.		5.83
I can successfully use it every time.		5.83
Learnability	Disagree 1 2 3 4 5 6 7 Agree	
I can learn to use it quickly.		5.63
I can easily remember how to use it.		5.75
It is easy to learn.		6.00
Soon I was able to use it proficiently.		5.92
Satisfaction	Disagree 1 2 3 4 5 6 7 Agree	
I am satisfied with it.		6.13
I would recommend it to friends.		5.63
Using it is enjoyable.		5.88
It works the way I hope.		5.79
It is good.		6.04
I feel that I need to own it.		5.33
Using it is pleasurable.		6.00

**Table 3.** USE questionnaire.

and create a prototype of a VR interaction product with therapeutic functions. VR technology provides users with an immersive embodied interaction experience, replacing the physical therapy rooms used in psychodrama with virtual game scenarios. The convenience of this interaction modality allows users to engage in the anxiety healing process from the comfort of their homes, experiencing virtual scenarios anytime and anywhere. The innovative expansion of the breathing interaction not only offers users a novel way to experience VR but also incorporates breathing therapy semantics that promote anxiety relief and enhance cardiopulmonary function. Data from the EEG user experiments and user experience reports confirm that this prototype effectively supports anxiety relief. Therefore, integrating VR interaction modalities with psychological healing can significantly simplify the process of anxiety treatment, facilitating timely and effective emotional regulation for users, which is of great importance in preventing anxiety disorders.

Limitations

At the hardware level, this study extended the existing modalities of virtual reality technology (visual, auditory, and haptic) by introducing an innovative breathing interaction modality, offering new possibilities for VR interaction methods. However, the hardware used in this study, including Arduino and respiratory detection sensors, represents a relatively basic level of integration. In future work, we will develop more integrated and advanced hardware technologies while exploring the extension and application of additional modalities.

At the software level, this study developed a breathing interaction system based on the Unreal Engine, currently featuring only three scenarios. While these scenarios correspond to three different breathing therapy techniques (diaphragmatic breathing, continuous exhalation, and breath-holding), the number of scenarios can be expanded, and the transitions between scenes, as well as the overall gaming experience, can be further

enhanced. In future work, we will focus on improving the interactive experience of the scenes and enriching the content of the interactions.

In the user experiment section, this study conducted a user experience and interactive therapy experiment with 38 participants. Throughout the experiment, participants wore EEG monitoring devices to collect data, and the effectiveness of the interactive therapy was validated through the analysis of Topographic Maps, Band-Power Reports, and ERP data. The EEG monitoring used a 16-channel device, yielding accurate and convincing data. However, incorporating additional multimodal detection devices, such as skin conductance and electrocardiogram (ECG) sensors, would further enhance the experimental results. In future work, we will consider employing more comprehensive human factor detection technologies to obtain even more precise monitoring data.

## Conclusion

Inspired by psychodrama therapy, this study constructs immersive, gamified interactive scenarios using virtual reality (VR) technology to embody users' emotions and inner world that they need to confront and engage with, providing an immersive, embodied, and convenient healing experience. Further inspired by breathing therapy, the study extends the breathing interaction modality within the VR system, designing an anxiety-focused breathing interaction method and semantics to enhance the therapeutic effectiveness of the immersive multimodal interaction system for anxiety relief. Beyond the mainstream VR interaction modalities—visual, auditory, and tactile—this study incorporates an olfactory (breathing) interaction modality to further enrich the overall VR experience. The innovative approach of exhalation (output) and inhalation (input) interaction within the olfactory modality breaks the conventional model of olfactory interaction, which primarily involves scent-based input, allowing users to actively participate rather than passively receive input during the healing process. This enhances the sense of realism and interactivity within the virtual environment. This research provides a reference for future innovative applications of VR and multimodal interaction technologies in studies focused on anxiety psychological healing methods.

## Data availability

The datasets used or analysed during the current study available from the corresponding author on reasonable request. Data access is restricted to research and educational applications.

Received: 20 March 2024; Accepted: 27 February 2025

Published online: 07 March 2025

## References

1. Craske, M. G. et al. What is an anxiety disorder? *Focus* **9**(3), 369–388 (2011).
2. American Psychiatric Association & Association, D. A. P. *Diagnostic and Statistical Manual of mental disorders: DSM-5* (American psychiatric association, 2013).
3. Zung, W. W. Self-rating anxiety scale. *BMC Psychiatry* (1971).
4. Li, W. et al. Prevalence and associated factors of depression and anxiety symptoms among college students: a systematic review and meta-analysis. *J. Child Psychol. Psychiatry*. **63**(11), 1222–1230 (2022).
5. Heimberg, R. G. Cognitive-behavioral therapy for social anxiety disorder: current status and future directions. *Biol. Psychiatry*. **51**(1), 101–108 (2002).
6. Goldin, P. R. & Gross, J. J. Effects of mindfulness-based stress reduction (MBSR) on emotion regulation in social anxiety disorder. *Emotion* **10**(1), 83 (2010).
7. Powers, M. B. & Emmelkamp, P. M. Virtual reality exposure therapy for anxiety disorders: A meta-analysis. *J. Anxiety Disord.* **22**(3), 561–569 (2008).
8. Krijn, M. et al. Virtual reality exposure therapy of anxiety disorders: A review. *Clin. Psychol. Rev.* **24**(3), 259–281 (2004).
9. Abbing, A. et al. The effectiveness of Art therapy for anxiety in adults: A systematic review of randomised and non-randomised controlled trials. *PLoS One*. **13**(12), e0208716 (2018).
10. Chambala, A. Anxiety and Art therapy: treatment in the public eye. *Art Therapy*. **25**(4), 187–189 (2008).
11. Jaynes, C. et al. The Metaverse: A networked collection of inexpensive, self-configuring, immersive environments. *Proceedings of the workshop on Virtual environments 2003* (2003).
12. Wang, X. et al. Reducing stress and anxiety in the metaverse: A systematic review of meditation, mindfulness and virtual reality. *Proceedings of the Tenth International Symposium of Chinese CHI* (2022).
13. Westheimer, G. Hermann Helmholtz and origins of sensory physiology. *Trends Neurosci.* **6**, 5–9 (1983).
14. Jewitt, C., Bezemer, J. & O'halloran, K. *Introducing Multimodality* (Routledge, 2016).
15. Lopez, D. S. *Elaborations on emptiness-uses of the Heart Sutra* (Princeton University Press, 1996).
16. Zimbardo, P. G. & Ruch, F. L. *Psychology and life* (1975).
17. Turk, M. Multimodal interaction: A review. *Pattern Recognit. Lett.* **36**, 189–195 (2014).
18. Kuriakose, B., Shrestha, R. & Sandnes, F. E. Multimodal navigation systems for users with visual impairments—a review and analysis. *Multimodal Technol. Interact.* **4**(4), 73 (2020).
19. Rosello, O. R. G. *HeartBit: Mindful Control of Heart Rate Using Haptic Biofeedback* (Massachusetts Institute of Technology, 2020).
20. Amores, J., Maes, P. & Essence Olfactory interfaces for unconscious influence of mood and cognitive performance. *Proceedings of the 2017 CHI Conference on Human Factors in Computing Systems* (2017).
21. Amores Fernandez, J. *Olfactory Interfaces: Toward Implicit human-computer Interaction across the Consciousness Continuum* (Massachusetts Institute of Technology, 2020).
22. Amores, J. et al. Bioessence: A wearable olfactory display that monitors cardio-respiratory information to support mental wellbeing. *Proceedings of the 2018 40th Annual International Conference of the IEEE Engineering in Medicine and (EMBC)* (IEEE, 2018).
23. Amores, J., Dotan, M. & Maes, P. An exploration of form factors for sleep-olfactory interfaces. *Proceedings of the 2019 41st Annual International Conference of the IEEE Engineering in Medicine and Biology Society (EMBC)* (IEEE, 2019).
24. Morris, C., Danry, V., Maes, P. & Ember A system for transfer of interoceptive sensations to improve social perception. *Proceedings of the 2022 ACM Designing Interactive Systems Conference* (2022).
25. Kosmyna, N. et al. AttentiVU: A wearable pair of EEG and EOG glasses for real-time physiological processing. *Proceedings of the 2019 IEEE 16th International Conference on Wearable and Implantable Body Sensor Networks (BSN)* (IEEE, 2019).



26. Jiang, F., Haddad, D. D. & Paradiso, J. Baguamarsh: An immersive narrative visualization for conveying subjective experience. *Proceedings of the Human-Computer Interaction Design and User Experience: Thematic Area, HCI 2020, Held as Part of the 22nd International Conference, HCII 2020, Copenhagen, Denmark, July 19–24, Proceedings, Part I 22* (Springer, 2020).
27. Bombari, D. et al. Studying social interactions through immersive virtual environment technology: virtues, pitfalls, and future challenges. *Front. Psychol.* **6**, 136009 (2015).
28. Kwon, D.-H. A study on the meanings of half-life: alyx and the success factors of VR games. *J. Korea Contents Association.* **20**(9), 271–284 (2020).
29. Jerreat-Poole, A. Virtual reality, disability, and futurity: Crippling technologies in Half-Life: alyx. *J. Literary Cult. Disabil. Stud.* **16**(1), 59–75 (2022).
30. Sanders, A. *An Introduction To Unreal Engine 4* (AK Peters/CRC, 2016).
31. Serial com plugin github page. [https://www.github.com/videofeedback/Unreal\\_Engine\\_SerialCOM\\_Plugin](https://www.github.com/videofeedback/Unreal_Engine_SerialCOM_Plugin).
32. Von Ameln, F., Gerstmann, R. & Kramer, J. *Psychodrama* (Springer, 2009).
33. Farokhi, M. Art therapy in humanistic psychiatry. *Procedia-Social Behav. Sci.* **30**, 2088–2092 (2011).
34. Pérez-Álvarez, M. Psychopathology according to behaviorism: A radical restatement. *Span. J. Psychol.* **7**(2), 171–177 (2004).
35. Foa E B. *Prolonged Exposure Therapy: Past, Present, and Future* (Depression and anxiety, 2011).
36. Freeman, D. et al. Automated virtual reality (VR) cognitive therapy for patients with psychosis: study protocol for a single-blind parallel group randomised controlled trial (gameChange). *BMJ Open.* **9**(8), e031606 (2019).
37. Freeman, D. et al. Automated virtual reality therapy to treat agoraphobic avoidance and distress in patients with psychosis (gameChange): a multicentre, parallel-group, single-blind, randomised, controlled trial in England with mediation and moderation analyses. *Lancet Psychiatry.* **9**(5), 375–388 (2022).
38. Cahalin, L. P. et al. Efficacy of diaphragmatic breathing in persons with chronic obstructive pulmonary disease: a review of the literature. *J. Cardiopulm. Rehabil. Prev.* **22**(1), 7–21 (2002).
39. Fernandes, M., Cukier, A. & Feltrim, M. I. Z. Efficacy of diaphragmatic breathing in patients with chronic obstructive pulmonary disease. *Chronic Resp. Dis.* **8**(4), 237–244 (2011).
40. Eherer, A. et al. Positive effect of abdominal breathing exercise on gastroesophageal reflux disease: a randomized, controlled study. *Official J. Am. Coll. Gastroenterology| ACG.* **107**(3), 372–378 (2012).
41. Zdrhova, L. et al. Breathing exercises in gastroesophageal reflux disease: a systematic review. *Dysphagia* **38**(2), 609–621 (2023).
42. Hamasaki, H. Effects of diaphragmatic breathing on health: a narrative review. *Medicines* **7**(10), 65 (2020).
43. Zou, L. et al. Effects of mind–body exercises (Tai Chi/Yoga) on heart rate variability parameters and perceived stress: A systematic review with meta-analysis of randomized controlled trials. *J. Clin. Med.* **7**(11), 404 (2018).
44. Lee, A. L., Burge, A. T. & Holland, A. E. Positive expiratory pressure therapy versus other airway clearance techniques for bronchiectasis. *Cochrane Database Syst. Rev.* **9** (2017).
45. Vatwani, A. Pursed lip breathing exercise to reduce shortness of breath. *Arch. Phys. Med. Rehabil.* **100**(1), 189–190 (2019).
46. Vannucci, R. C. et al. Carbon dioxide protects the perinatal brain from hypoxic-ischemic damage: an experimental study in the immature rat. *Pediatrics* **95**(6), 868–874 (1995).
47. Kashiwagi, K. et al. The effects of reactive oxygen species on amphibian aging. *Comp. Biochem. Physiol. C: Toxicol. Pharmacol.* **140**(2), 197–205 (2005).
48. Bouten, J., Bourgois, J. G. & Boone, J. Hold your breath: peripheral and cerebral oxygenation during dry static apnea. *Eur. J. Appl. Physiol.* **120**, 2213–2222 (2020).
49. Jerath, R. et al. Self-regulation of breathing as a primary treatment for anxiety. *Appl. Psychophysiol. Biofeedback.* **40**(2), 107–115 (2015).
50. Liu, X. *Inward To Outward* (Massachusetts Institute of Technology, 2017).
51. Rifqah, R. A. N. et al. Design of a classroom noise monitoring tool using a KY-037 sound sensor based on Wemos D1R1. *J. Energy Mater. Instrum. Technol.* **4**(4), 125–135 (2023).
52. Wang, H. et al. The power spectrum and functional connectivity characteristics of resting-state EEG in patients with generalized anxiety disorder. *Sci. Rep.* **15**(1), 5991 (2025).
53. Stewart, J. L. et al. Frontal EEG asymmetry during emotional challenge differentiates individuals with and without lifetime major depressive disorder. *J. Affect. Disord.* **129**(1–3), 167–174 (2011).
54. Palmiero, M. & Piccardi, L. Frontal EEG asymmetry of mood: A Mini-Review. *Front. Behav. Neurosci.* **11** (2017).
55. Metzen, D. et al. Frontal and parietal EEG alpha asymmetry: a large-scale investigation of short-term reliability on distinct EEG systems. *Brain Struct. Function.* **227**(2), 725–740 (2022).
56. Monni, A. et al. The novel frontal alpha asymmetry factor and its association with depression, anxiety, and personality traits. *Psychophysiology* **59**(11), e14109 (2022).
57. Dunstan, D. A. & Scott, N. Norms for Zung’s self-rating anxiety scale. *BMC Psychiatry.* **20**, 1–8 (2020).
58. Delorme, A. & Makeig, S. EEGLAB: an open source toolbox for analysis of single-trial EEG dynamics including independent component analysis. *J. Neurosci. Methods.* **134**(1), 9–21 (2004).
59. Luck, S. J. *An Introduction To the event-related Potential Technique* (MIT Press, 2014).
60. Polich, J. Updating P300: an integrative theory of P3a and P3b. *Clin. Neurophysiol.* **118**(10), 2128–2148 (2007).
61. Harmon-Jones, E. & Gable, P. A. On the role of asymmetric frontal cortical activity in approach and withdrawal motivation: an updated review of the evidence. *Psychophysiology* **55**(1), e12879 (2018).

## Acknowledgements

We extend our sincerest gratitude to all participants involved in the human-computer interaction and EEG testing experiments conducted for this study. We also express our appreciation to the funding support by the R&D Program of Beijing Municipal Education Commission under Grant SM202310005009.

## Author contributions

Conceptualization, S.Z., L.C.; Methodology, S.Z., L.C.; Validation, S.Z., L.C., and S.L.; Investigation, S.Z., L.C.; Experiment, S.Z., L.C., and S.L.; Writing—original draft, S.Z., L.C., and S.L.; Writing—review and editing, S.Z., S.L.; Supervision, S.Z.; Project administration, S.Z.; Funding acquisition, S.Z. All authors have read and agreed to the published version of the manuscript.

## Declarations

## Competing interests

The authors declare no competing interests.



### Ethical approval

This work involved human subjects in its research. Approval of all ethical and experimental procedures and protocols was granted by the Science and Technology Ethics Committee of Beijing University of Technology. All methods were carried out in accordance with relevant guidelines and regulations.

### Informed consent

The author confirmed that detailed information about this research and experimental procedures has been thoroughly explained to all experiment participants and notifying them that the results of this study will be published in the academic paper. Images of participants from the experimental process may appear in the research manuscript, which may contain certain identifiable features. Written informed consent for both experiment participation and images publication were obtained from each participant.

### Additional information

**Correspondence** and requests for materials should be addressed to S.Z.

**Reprints and permissions information** is available at [www.nature.com/reprints](http://www.nature.com/reprints).

**Publisher's note** Springer Nature remains neutral with regard to jurisdictional claims in published maps and institutional affiliations.

**Open Access** This article is licensed under a Creative Commons Attribution-NonCommercial-NoDerivatives 4.0 International License, which permits any non-commercial use, sharing, distribution and reproduction in any medium or format, as long as you give appropriate credit to the original author(s) and the source, provide a link to the Creative Commons licence, and indicate if you modified the licensed material. You do not have permission under this licence to share adapted material derived from this article or parts of it. The images or other third party material in this article are included in the article's Creative Commons licence, unless indicated otherwise in a credit line to the material. If material is not included in the article's Creative Commons licence and your intended use is not permitted by statutory regulation or exceeds the permitted use, you will need to obtain permission directly from the copyright holder. To view a copy of this licence, visit <http://creativecommons.org/licenses/by-nc-nd/4.0/>.

© The Author(s) 2025